JOURNAL OF MATERIALS SCIENCE 20 (1985) 2011–2022

Multicomponent toughened ceramic materials obtained by reaction sintering

Part 1 ZrO_2–Al_2O_3–SiO_2–CaO system

P. PENA, P. MIRANZO, J. S. MOYA, S. DE AZA
Instituto de Cerámica y Vidrio (C.S.I.C.), Arganda del Rey, Madrid, Spain

Fully dense zirconia toughened ceramics with a mullite matrix from the basis of information on the quaternary system ZrO_2–Al_2O_3–SiO_2–CaO, in a temperature range as low as 1425 to 1450° C, have been obtained by reaction sintering of zircon/alumina/calcium carbonate mixtures. The shrinkage, advance of reaction, microstructure and mechanical properties of different compositions are reported. The results are explained in terms of a transitory liquid phase that appears at temperatures lower than 1400° C.

1. Introduction

Reaction sintering (RS) of mixed fine zircon-based powders is a route [1, 2] for producing ceramics containing dispersed zirconia grains with enhanced mechanical properties. The RS between zircon and alumina to produce zirconia toughened mullite according to:

$$\underset{\text{zircon}}{2ZrSiO_4} + 3Al_2O_3 \rightarrow 2ZrO_2 + \underset{\text{mullite}}{3Al_2O_3 \cdot 2SiO_2} \quad (1)$$

has been extensively studied. In order to obtain fully dense zirconia toughened mullite, two different firing procedures have been used: the first separates the densification and reaction steps [1, 3], whereas the second utilizes RS aids in order to perform the reaction (production of dispersed ZrO_2), and the densification of the ceramic occurs simultaneously [4]. Both procedures lead to mullite with flexural strengths, σ_f, $\sim 400\,MN\,m^{-2}$ and fracture toughness, K_{IC}, $\sim 4.5\,MN\,m^{-3/2}$ suggesting that considerable toughening in this material is possible.

However, in the case of zircon and alumina mixtures in stoichiometric proportions corresponding to Reaction 1, in order to obtain full density and complete reaction, a complex processing is required: i.e. high isostatic pressure (630 MPa) and two thermal heating steps at 1400 and 1600° C [1–3].

One method available for reducing the firing temperature is the use of additives which can act as sintering aids; these can be broadly classified under three different headings, (1) permanent liquid phase sintering additives, (2) solid solution additives, and (3) transitory liquid phase sintering additives.

A number of liquid phase additives have been recognized as allowing a reduction in the required temperature of sintering. However, the intergranular phases which are brought about by the preence of this kind of additive, usually causes some degradation of the mechanical properties of the product.

In contrast, the use of solid solution additives avoids the appearance of an extra-phase problem, and at the same time allows significant modifications in the pattern of microstructural development during sintering.

The aim of the present work is to obtain zirconia toughened materials by RS on the basis of information supplied by the quaternary systems ZrO_2–Al_2O_3–SiO_2–XO (X = Ca, Mg, Ti) in order to facilitate processing as well as densification procedure.

The first part of this work concerns the effect of CaO additions on the RS of zircon/alumina mixtures.

2. Phase equilibria diagram ZrO_2–Al_2O_3–SiO_2–CaO

In Fig. 1 the zirconia solid-state compatibility relationships in the quaternary system

0022–2461/85 $03.00 + .12

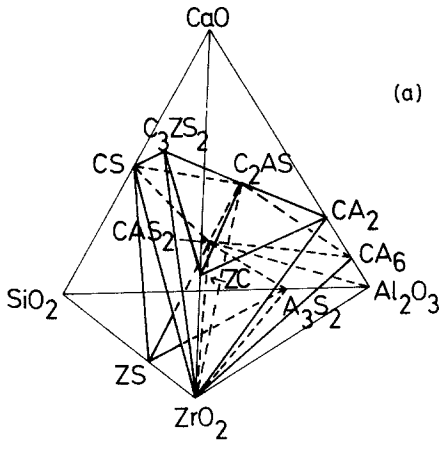

Figure 1 (a) Solid-state compatibility relationships in the ZrO_2–Al_2O_3–SiO_2–CaO system. (b) Projection through ZrO_2-corner showing secondary phases crystallizing during freezing from ZrO_2–Al_2O_3–SiO_2–CaO mixtures containing 60 wt % ZrO_2. The various symbols, ✲, ✿, ■, represent experimental compositions.

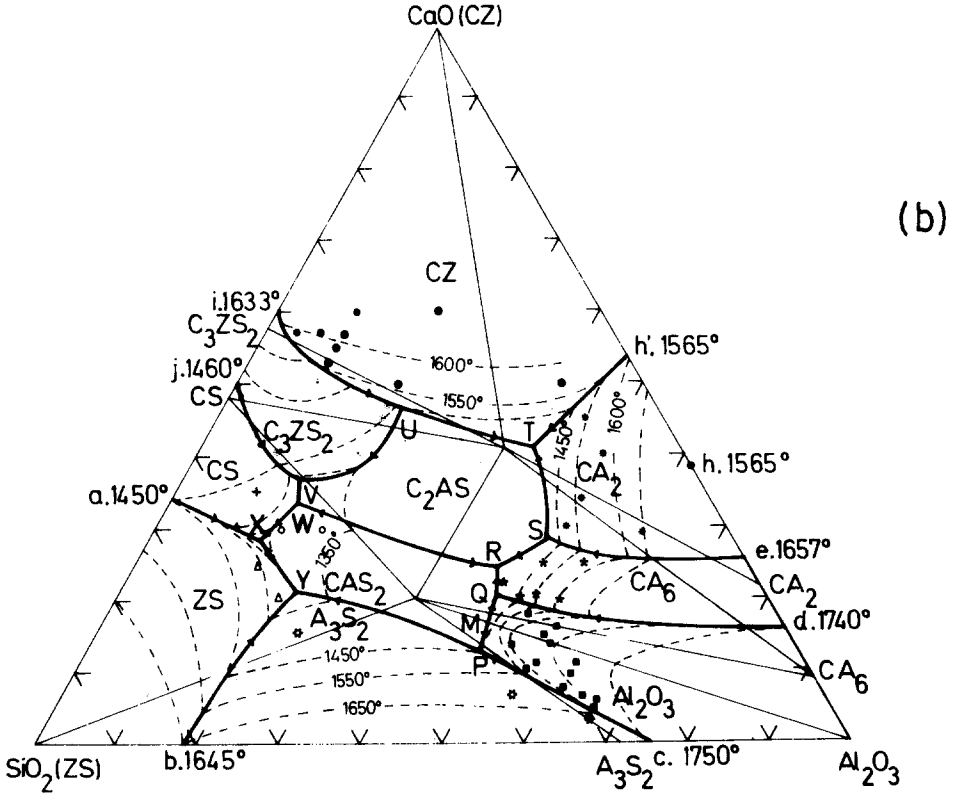

ZrO_2–Al_2O_3–SiO_2–CaO, and the projection of the primary phase volume of zirconia from the zirconia corner on to the opposite face of the composition tetrahedra are shown [5, 6].

Taking into account the zirconia solid-state compatibility relationships, and the experimental results obtained in previous work [4], $ZrSiO_4$/Al_2O_3/CaO compositions with the following molar proportion were studied:

$$(2 + 2x)\,ZrSiO_4 + 3Al_2O_3 + x(CaO + Al_2O_3)$$

These compositions lie in the solid-state compatibility plane zirconia–mullite–anorthite and are located in the straight line a–b (Fig. 2) defined by

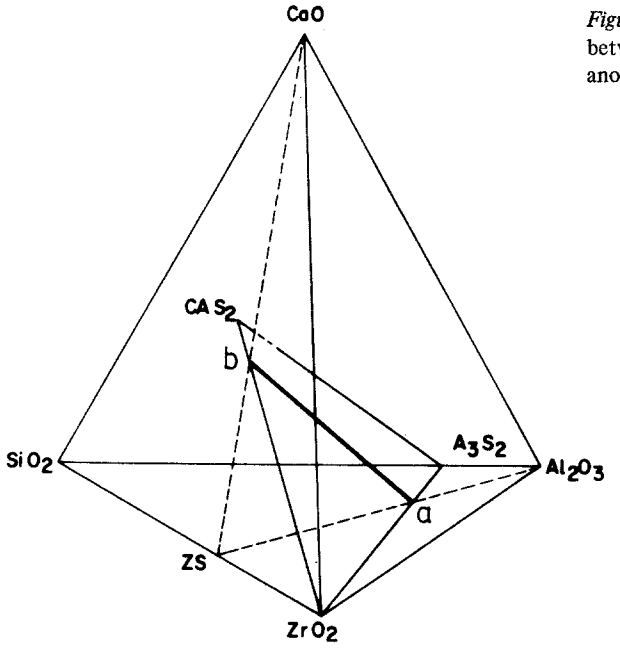

Figure 2 Diagrammatic representation of the intersection between the solid state compatibility zirconia–mullite–anorthite plane and the $ZrSiO_4 - Al_2O_3 - CaO$ plane.

the equation:

$$(2 + 2x)\underset{\text{zircon}}{ZrSiO_4} + 3Al_2O_3 + x(Al_2O_3 + CaO) \rightarrow$$

$$(2 + 2x)ZrO_2 + \underset{\text{mullite}}{Al_6Si_2O_{13}} + x\underset{\text{anorthite}}{CaAl_2Si_2O_8} \quad (2)$$

According to the system ZrO_2–Al_2O_3–CaO–SiO_2, for all these compositions the initial liquid formation starts at ~ 1440° C, invariant point of the subsystem zirconia–alumina–mullite–anorthite.

From the projection of the primary phase volume of ZrO_2, from the zirconia corner on to the opposite face of the composition tetrahedron (Fig. 1) it can be stated that the two compositions considered ($x = 0.37$; $x = 1$) are located in the primary field of ZrO_2, while in the case of the secondary phase it may be deduced that for CaO contents higher than ~ 4 wt% the secondary phase that appears is Al_2O_3, and for contents lower than this value the corresponding phase is mullite. At temperatures slightly higher than that of the invariant point (1440° C), three phases ZrO_2, Al_2O_3, and mullite coexist with a liquid phase.

An important feature of the system is the evidence that solid solutions of CaO in ZrO_2 are not stable in the presence of alumina as has been proved by Pena and de Aza in previous work [5].

3. Experimental details

3.1. Materials

The raw materials used were zircon opacifier supplied by Quiminsa, (Opazir S), a finely milled mineral zircon, Fluka (99.998%) low-sodium Al_2O_3, and CaO produced by calcination of reagent grade $CaCO_3$ Merk at 900° C for 2 h. The manufacturer's specification showed that the major impurities in the zircon were Al_2O_3 0.9 wt%, TiO_2 0.2 wt% and Fe_2O_3 0.1 wt%. The quoted initial specific surface area measured by BET was found to be 5.4 $m^2 g^{-1}$, and grain size distribution curves determined by the sedigraph method were found to have a mean grain size diameter of 1.35 μm and the shape of the curve is shown to be the result of milling operations.

3.2. Firing and sample preparation

The $ZrSiO_4/Al_2O_3/CaO$ compositions were performed according to the molar proportion of Equation 2 where x ranges from 0 to 1. The mixtures were homogenized by attrition milling in isopropyl alchohol media for 1 h. After drying and sieving the powders were isostatically pressed into bars (~ 5mm diameter), at 200 MPa.

The specimens were fired in an electric temperature controlled furnace, heated by Kanthal elements, in the temperature interval from 1425 to 1500° C.

3.3. Density measurements

Water and bulk mercury displacement methods were both used to measure the bulk density of the samples; the mercury method was applied in the case of the green samples. The theoretical densities were calculated taking into account the phase compositions of the products as well as the true density values of zircon (4.68 $Mg\,m^{-3}$), zirconia (t) (6.10 $Mg\,m^{-3}$), zirconia (m) (5.83 $Mg\,m^{-3}$), anorthite (2.76 $Mg\,m^{-3}$) and CaO (3.345 $Mg\,m^{-3}$).

3.4. Dilatometric measurement

The shrinkage evolution as a function of temperature has been studied on samples with $x = 0$ and $x = 1$ of ~5 mm length in a Stanton Redcorft dilatometric apparatus with a constant heating rate of 10° C min^{-1} up to 1500° C.

3.5. X-ray analysis

After firing, the samples were air-quenched and a portion of each one was ground to a particle size $<35\,\mu m$ and examined by X-ray diffraction on a Philips 1010 diffractometer with a nickel filter and Cu$K\alpha$ radiation; the scanning speed used was 2 or $\frac{1}{2}$ $2\Theta\,min^{-1}$. The areas of the peaks (1 1 1) and (1 1 $\bar{1}$) of monoclinic zirconia, (1 1 1) of tetragonal zirconia, (2 0 0) of zircon, (1 1 3) of α-alumina and (1 1 0) of mullite were used in the quantitative analysis.

The bulk retained t-ZrO_2 fraction (x_t) was determined on polished samples and as-sintered samples using the Garvie–Nicholson [7] relationship

$$x_t = \frac{I_{1\,1\,1}(t)}{I_{1\,1\,1}(t) + I_{1\,1\,1}(m) + I_{1\,1\,\bar{1}}(m)}$$

The extent of the chemical Reaction 2 was estimated in terms of two parameters α and β. The α parameter was defined as the ratio

$$\alpha = \frac{C_z}{C_z + C_{zs}} \tag{3}$$

where C_z and C_{zs} are the concentrations of zirconia and zircon, respectively; α gives the value of zircon dissociation. The β parameter was defined as:

$$\beta = \frac{C_M}{C_M + C_A} \tag{4}$$

where C_M and C_A are the concentrations of mullite and alumina, respectively. This parameter is related to the formation of mullite.

It is known that [8]:

$$I_z = K_1 \frac{C_z}{\mu_T}; I_{zs} = K_2 \frac{C_{zs}}{\mu_T} \tag{5}$$

where μ_T is the mass absorption coefficient of the samples; K_1 and K_2 are constants and I_z, I_{zs} correspond to the previously mentioned m-ZrO_2 (1 1 1) and $ZrSiO_4$ (2 0 0) diffraction lines intensities.

Dividing I_{zs} by I_z, the μ_T coefficient can be eliminated:

$$\frac{I_{zs}}{I_z} = K \frac{C_{zs}}{C_z} \tag{6}$$

Taking into account Equations 3 and 6

$$\alpha = \frac{1}{1 + (1/K)(I_{zs}/I_z)} \tag{7}$$

Similarly:

$$\beta = 1/[1 + (1/K')(I_A/I_M)]$$

It should be noted that α and β can vary between 0 and 1.

The values of K and K' were determined from the calibration curves obtained from X-ray diffraction patterns of zircon and baddeleyite mixtures and α-alumina and mullite mixtures. Mullite powder was obtained from calcined Kaolinite at 1500° C using the method of Demidova and Goucharov [9].

In Fig. 3a the ratio of the area of the X-ray peak of zircon to that of zirconia (m) is plotted against C_{zs}/C_z. As can be expected according to Chung [10–12] a straight line is obtained. From the slope of this line the value of K was determined to be 1.232 ± 0.001.

Similarly, in Fig. 3b, the ratio I_A/I_M as a function of C_A/C_M is plotted and the value of K' obtained was 2.94 ± 0.01.

3.6. Microstructural analysis

The microstructure of the samples has been studied by SEM (ISI 130) and by energy dispersive X-ray microanalysis (Kevex 7030) on polished surfaces (a) thermally etched at 1350° C/2 h and (b) chemically etched by HF (10%)/15 sec.

3.7. Mechanical properties

The bend strength (σ_f) and the critical stress

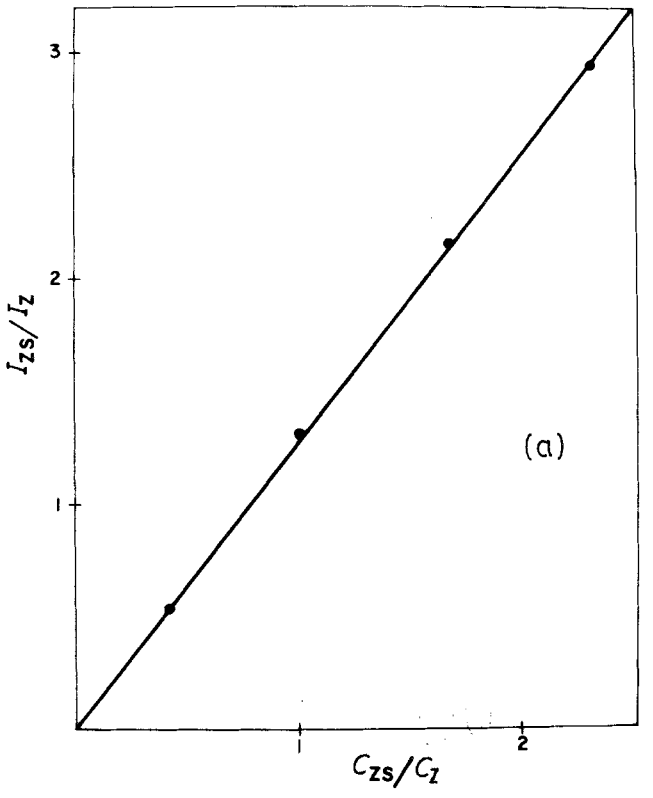

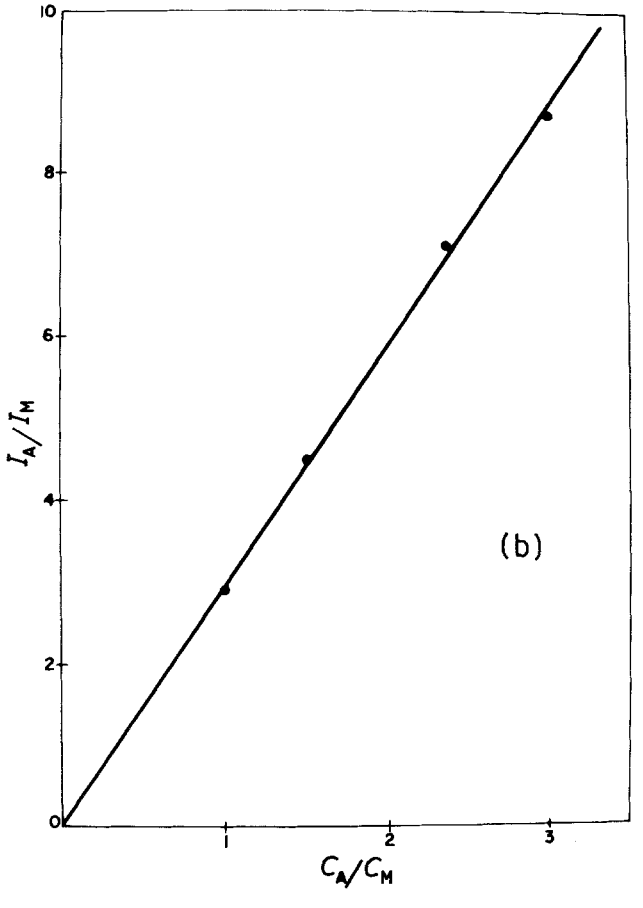

Figure 3 Plots of the fit for (a) I_{zs}/I_z against C_{zs}/C_z, and (b) I_A/I_M against C_A/C_M.

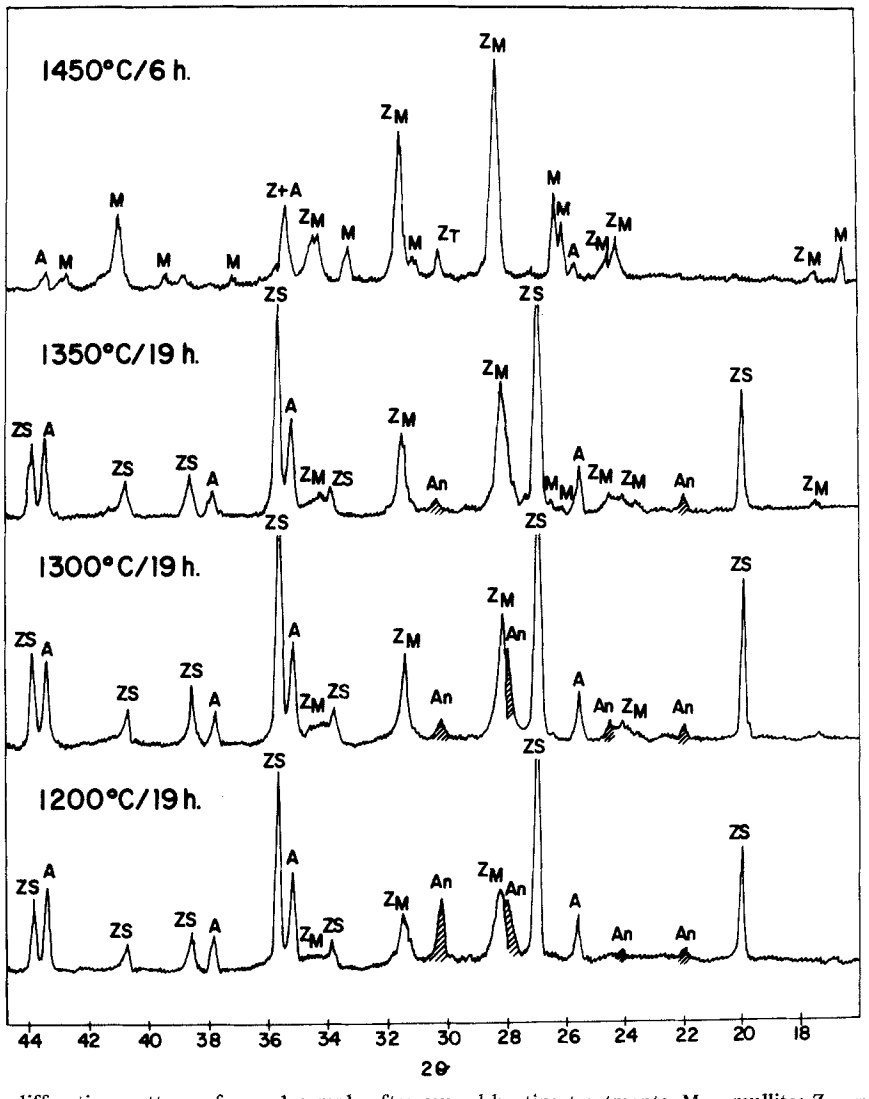

Figure 4 X-ray diffraction pattern of $x = 1$ sample after several heating treatments. M = mullite; Z_M = m-ZrO_2; Z_T = t-ZrO_2; ZS = $ZrSiO_4$ and An = $CaAl_2Si_2O_8$.

intensity factor (K_{IC}) have been determined by three point bending and by indentation method [13], respectively, using an Instron machine and a reflected light microscope.

4. Results and discussion

In the densification of reacting powder systems two phenomena occur: porosity removal and reaction. Consequently, the control of the rate at which each of these phenomena takes place is the first stage to achieve the desired microstructures and properties of RS materials. On the compositions studied in the present work, the reactant densities are higher than those of the final products; hence the porosity removal tends to reduce the specimen dimension while the reaction has the opposite effect. In this way it is preferable to complete porosity removal prior to the reaction in order to obtain fully dense samples with a zirconia dispersed phase. Conversely, if reaction precedes porosity removal, the heat treatment required to eliminate the pores also allows the zirconia grains to grow, thus it is more difficult to control microstructure and consequently mechanical properties.

In order to determine the sintering reaction sequence, green compact samples were heated at temperatures ranging from 1200 to 1450° C for different times.

In Fig. 4 the X-ray diffraction patterns cor-

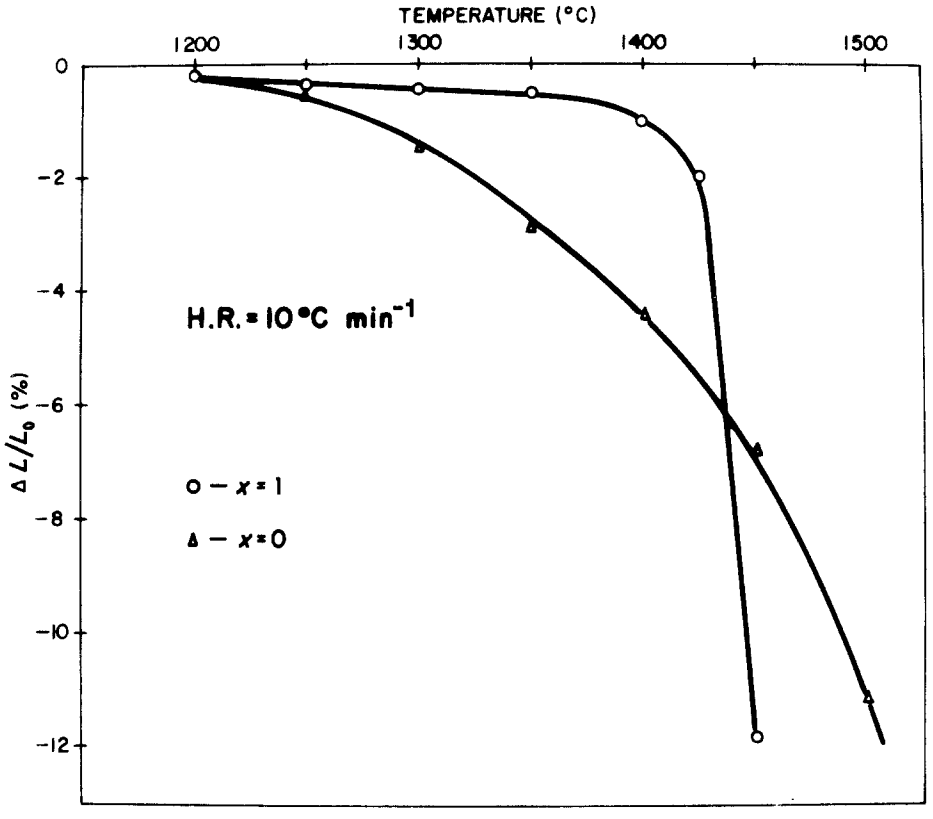

Figure 5 Shrinkage of $x = 0$ and $x = 1$ samples as a function of temperature.

responding to the $x = 1$ sample are shown. At 1200° C, anorthite ($CaAl_2Si_2O_8$) coexisting with zircon, zirconia and alumina was detected; between 1200 and 1350° C the anorthite content decreases and the zircon dissociation increases slowly; at higher temperature (1450° C) the expected equilibrium phase (zirconia, mullite and alumina) are present.

The coexistence of anorthite with zircon and zirconia suggests the possibility of a small amount of liquid phase appearing at the temperature of the invariant point ZrO_2–$CaAl_2Si_2O_8$–$ZrSiO_4$–$CaSiO_3$ (~ 1200° C) (Fig. 1b). This non-equilibrium situation can progress towards the corresponding equilibrium phases ($ZrO_2 + Al_6Si_2O_{13} + CaAl_2Si_2O_8$) in two steps: (a) following the boundary $ZrO_2 + ZrSiO_4 + CaAl_2Si_2O_8$ + liq to the invariant point zircon + zirconia + mullite + anorthite + liq, and (b) following the boundary zirconia + mullite + anorthite + liq to reach the final peritectic equilibrium point zirconia–mullite–anorthite (1440° C). At higher temperatures, anorthite disappears and a permanent liquid phase is present together with Al_2O_3, mullite and zirconia.

In Fig. 5 shrinkage ($\Delta l/l_0$) as a function of temperature for the two compositions $x = 0$ and $x = 1$ is plotted. As can be observed from this figure the shrinkage behaviour of both samples is quite different. While for sample $x = 0$ the shrinkage starts at 1250° C and continues monotonically (see Part 2 of this study), for sample $x = 1$ two steps can be clearly appreciated: (1) between 1250 and 1400° C a smooth contraction is observed, and (2) at 1400° C this contraction suddenly increases. This curve can be considered as the typical one for a liquid phase sintering. A similar behaviour was observed by Huppmann *et al.* [14] in the system Al_2O_3–anorthite where a liquid phase appears at temperatures close to 1450° C. The temperature at which the shrinkage starts (~ 1250° C) is very close to that of the invariant point $ZrSiO_4$, ZrO_2, CAS_2, CS [6]. This liquid phase can be considered as a transitory liquid which would enhance the sintering rate. Over the peritectic point temperature of the system ZrO_2–mullite–anorthite, a permanent liquid phase appears; consequently a liquid phase sintering takes place, which produces a change in the slope of the shrinkage curve (Fig. 5).

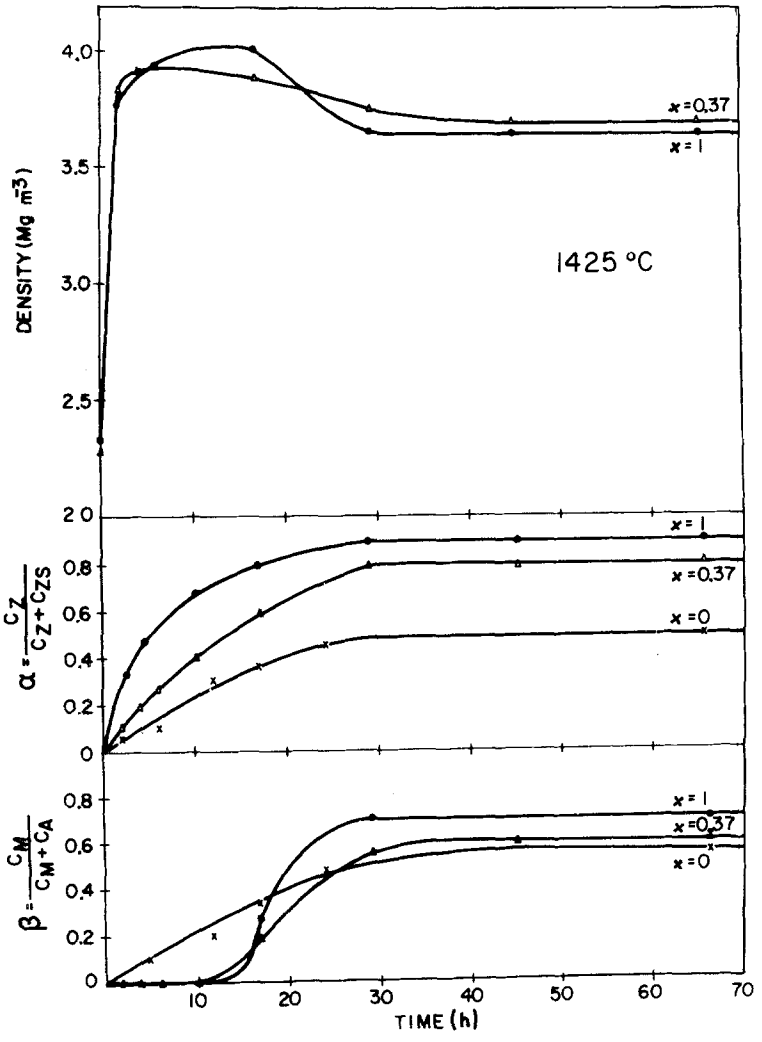

Figure 6 Evolution of densification, α and β for compositions $x = 0$, 0.37 and 1 as a function of time, at 1425° C.

The fact that the shrinkage for $x = 1$ composition is almost negligible up to ~ 1400° C can be explained by the formation of anorthite at the necks of the grains as has been detected after heating at 1200° C by X-ray diffraction. Anorthite has a density (2.76 Mg m^{-3}) significantly lower than that corresponding to the rest of the other components (3.803 Mg m^{-3}), and consequently acts with an expansive effect.

Taking into account the dilatometric curve of Fig. 6, a kinetic study has been made at temperatures higher than 1400° C.

In Fig. 6 the evolution of Reaction 2 as well as the densification process for $x = 0$, $x = 0.37$ and $x = 1$ at 1425° C is shown.

The following points are noticeable: (1) the rate of Reaction 2 is significantly higher in the case of samples with $x > 0$ than in the case $x = 0$; (2) the reaction of dissociation of zircon is faster than the reaction of formation of mullite, e.g. after 10 h at 1425° C, $\beta = 0$ while the value of $\alpha > 40\%$, at 30 h treatment the amount of mullite detected is $> 50\%$. A similar behaviour was observed by Pena *et al.* [4] in 3ZS/A/M mixtures treated at 1425° C; (3) from the densification curves two steps are clearly observed; first, sintering of the reactants and secondary reactions.

As has been previously stated [15] a small volume fraction of liquid affects the particle rearrangement and consequently enhances the initial stage of sintering. The presence of a transitory liquid phase at ~ 1250° C in the case of CaO-containing samples plays an important role in the reaction-sintering process.

In Figs. 7 and 8 the effect of temperature on Reaction 2 and densification is shown. From these

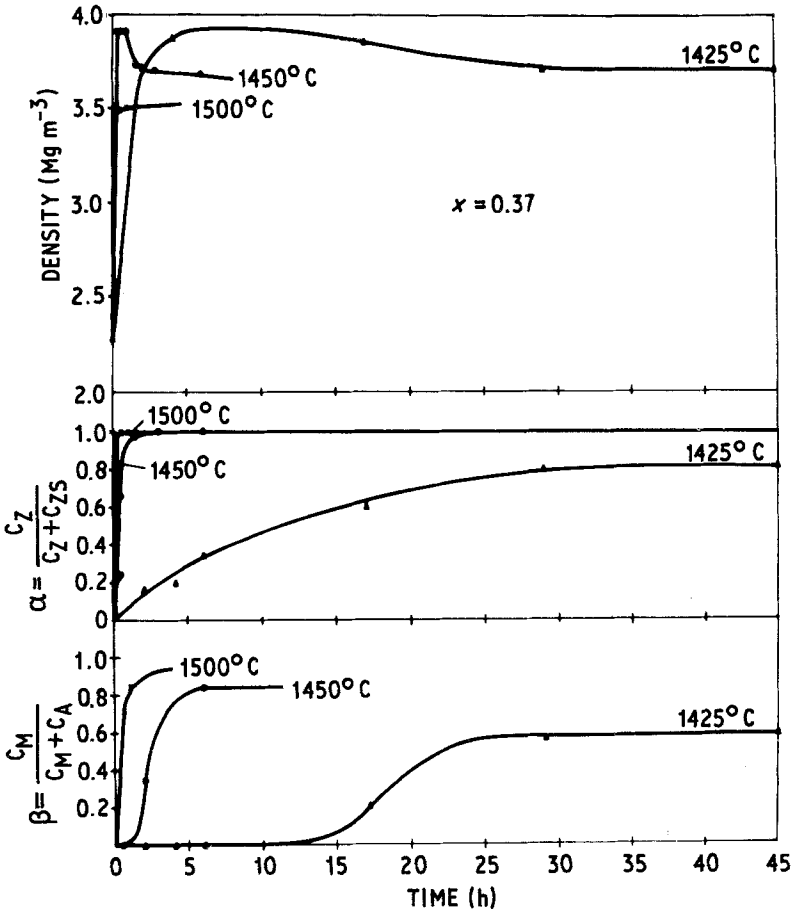

Figure 7 Densification and reaction rate for the composition $x = 0.37$ against time at different temperatures.

figures it can be deduced that the rate of reaction is very temperature dependent, i.e. at 1450° C after 3 h treatment all zircon has been dissociated, at this time the mullite reaches the maximum value, while only 25° C below, this phenomena required almost 30 h.

It can be noticed that the rate of porosity removal as well as reaction is much higher when the temperature overpasses the peritectic temperature (1440° C) of the subsystem ZrO_2–mullite–Al_2O_3–anorthite (Fig. 1); this is due to the appearance (i.e. 1450° C) at the equilibrium of a small amount of permanent liquid.

Fig. 9 shows examples of the microstructures of the sintered specimens at several magnifications. As a consequence of the higher atomic number of zirconium, zirconia particles differ clearly from their surrounding mullite matrix under observation by SEM in showing a brighter image.

Two kinds of zirconia particles are observed: – one, named intragranular, has a very small particle size ($< 1\,\mu m$) and spherical shape; the other one, intergranular, has a higher mean particle size (1 to $2\,\mu m$) and quasi-cubic shape. The residual pores are primarily intergranular.

The mullite grains have a columnar shape with a square section and dimensions ranging from 5 to $10\,\mu m$ length and 1 to $2\,\mu m$ width. This mullite crystal shape shows that the mullite crystal has grown in the presence of a liquid phase, as can be observed in SEM micrographs obtained on HF etched samples (Fig. 10).

The intergranular quasi-cubic ZrO_2-grains are surrounded by a small amount of liquid phase. This fact can explain the differences found in the size of both families of ZrO_2 grains.

In the case of intergranular-ZrO_2, the grains grow by a Ostwald ripening mechanism through a liquid phase. Conversely, in the case of intragranular ZrO_2, the particles grow by solid state diffusion through the mullite lattice. Obviously the former mechanism is faster than the latter, and consequently a larger average size is expected for intergranular-ZrO_2 particles, as observed.

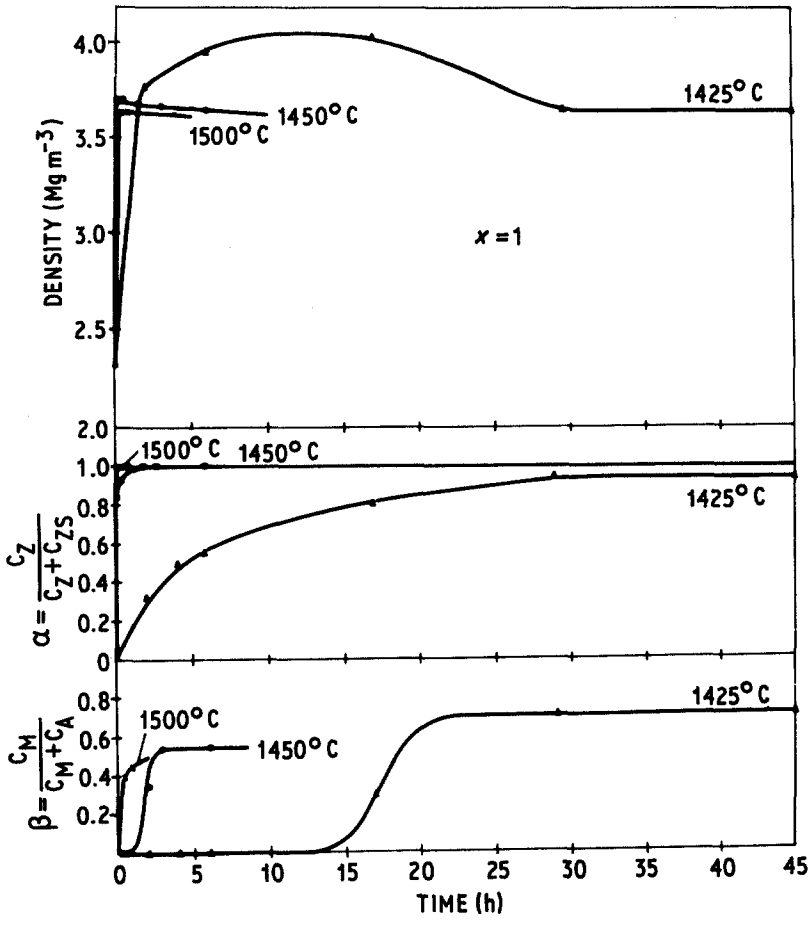

Figure 8 Densification and reaction rate for $x = 1$ against time at different temperatures.

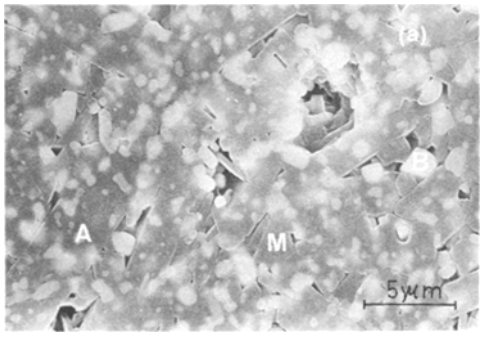

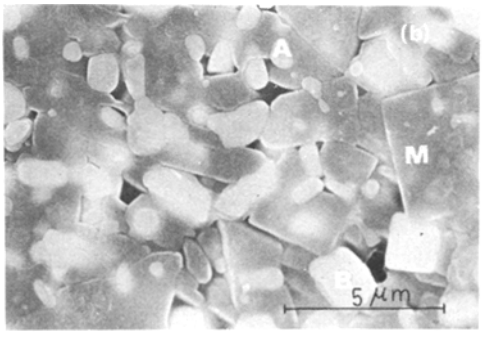

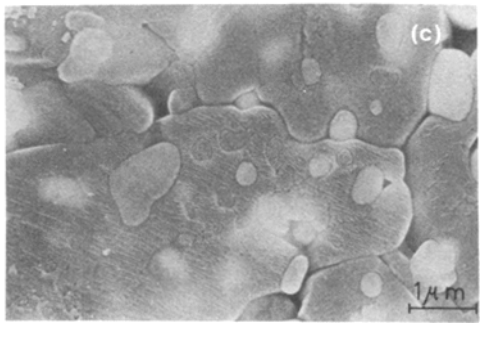

Figure 9 (a) Microstructure of the sample with $x = 1$ after 2 h at 1450° C. (b) Details of zirconia–mullite composite sintered at 1450° C. A = zirconia-intragranular, B = zirconia-intergranular and M = mullite. (c) A high magnification micrograph of the same sample.

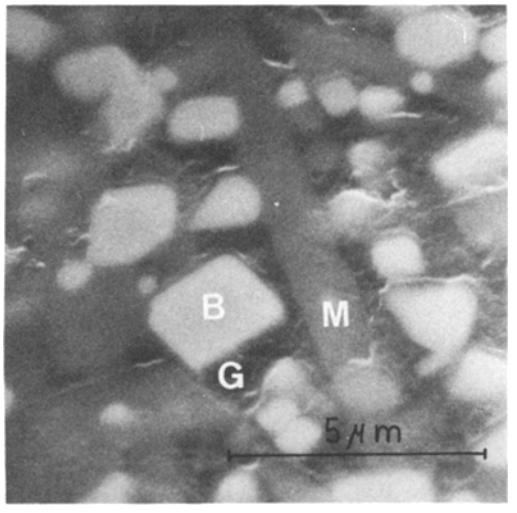

Figure 10 SEM picture of $x = 1$ sample chemically etched showing glassy phase. M = mullite, B = zirconia-intergranular and G = glassy phase.

An extensive study of this phenomenon has been made by Leriche *et al.* [16] on MgO-containing samples.

In the case of samples with $x = 1$ heated at 1450° C, 10° C over the temperature of the invariant point corresponding to the system ZrO_2–mullite–anorthite–alumina, a small permanent amount of liquid phase appears, as detected by chemical etching. In Fig. 9c a high magnification scanning electron micrograph of an $x = 1$ sample microstructure heated at 1450° C/2 h is shown. In this micrograph small inclusions of alumina grains ~1 μm are observed. Alumina is a stable phase at the mentioned temperature as can be deduced from Fig. 1b.

The relative t-ZrO_2 contents (x_t), σ_f and K_{IC} for $x = 0.37$ and $x = 1$ compositions after different thermal treatments are shown in Table I. The K_{IC} values determined in the different samples studied (~4.3 MPa $m^{1/2}$) is significantly higher than that corresponding to pure sintered mullite (~2 MPa $m^{1/2}$). A similar trend is observed in the modulus of rupture (σ_f). The difference between the σ_f corresponding to $x = 0.37$ (270 MPa) and that corresponding to $x = 1$ (230 MPa) can be explained by the relatively higher contents of glassy phase in the sample $x = 1$ heated at 1450° C.

The value of K_{IC} for the different samples can be considered independent of the zirconia tetragonal fraction as well as of the heating treatment. The t-ZrO_2 fraction has been found to be very low (<10%) in almost all samples studied. These facts suggested that the toughening mechanism operating in these multicomponent composites may be similar to that proposed by Moya and co-workers [17, 18], by metastable solid solution at the grain boundary as observed in mullite/ZrO_2 composites obtained by conventional sintering. However, taking into account the complex microstructure of these multicomponent composites, other possible contributions must be considered.

References

1. N. CLAUSSEN and J. JAHN, *J. Amer. Ceram. Soc.* **63** (1980) 228.
2. M. R. ANSEAU, C. LEBLUD and F. CAMBIER, *J. Mater. Sci. Lett.* **2** (1983) 366.
3. J. S. WALLACE, G. PETZON and N. CLAUSSEN, *Adv. Ceram.* **11** (1984), in press.
4. P. PENA, J. S. MOYA, S. DE AZA, ED. CARDINAL, F. CAMBIER, C. LEBLUND and M. R. ANSEAU, *J. Mater. Sci. Lett.* **2** (1983) 772.
5. P. PENA and S. DE AZA, *J. Amer. Ceram. Soc.* **1** (1984) C3–C5.
6. *Idem*, *Adv. Ceram.* **11** (1984), in press.
7. R. C. GARVIE and P. S. NICHOLSON, *J. Amer. Ceram. Soc.* **55** (1972) 303.
8. H. P. KLUG and L. E. ALEXANDER, "X-ray Diffraction Procedures" (Wiley, New York, 1954).
9. L. D. DEMIDOVA and GOUCHAROV, *Ogneupory* **20** (1955) 181.

TABLE I

Composition (mol)	T(° C)	t(h)	x_t(%)	σ_f^*(MPa)	K_{IC}(MPa $m^{1/2}$)
4ZS/4A/C	1425	45	4	–	4.2 ± 0.1
	1450	2	20	235 ± 30	4.3 ± 0.1
	1450	3	12	–	4.3 ± 0.1
2.74ZS/3.37A/0.37C	1425	45	4	–	4.1 ± 0.1
	1450	2	5	270 ± 15	4.4 ± 0.1
	1450	3	8	–	4.4 ± 0.1

*Average value over 5 measurements. ZS = $ZrSiO_4$; A = Al_2O_3; C = CaO

10. F. H. CHUNG, *J. Appl. Cryst.* 7 (1974) 519.
11. *Idem, ibid.* 7 (1974) 526.
12. *Idem, ibid.* 8 (1975) 17.
13. P. MIRANZO and J. S. MOYA, *Int. Ceram.*, in press.
14. W. J. HUPPMANN and H. RIEGGER, *Sci. Ceram* 9 (1977) 67.
15. R. PAMPUCH, "Ceramic Materials" (Elsevier; Amsterdam, 1976) p. 147.
16. A. LERICHE, L. DAPRA, M. R. ANSEAU, C. LEBLUD and F. CAMBIER, Proceedings of the 2nd Irish Durability and Fracture Conference, Limerick, March, 1984, to be published.
17. J. S. MOYA and M. I. OSENDI, *J. Mater. Sci. Lett.* 2 (1983) 500.
18. T. R. DINGER, K. M. KRISHNAN, G. THOMAS, M. I. OSENDI and J. S. MOYA, *Acta Metall.* 32 (1984) 1601.

Received 25 June
and accepted 6 July 1984